Topological gauge field in nanomagnets: Spin-wave excitations over a slowly moving magnetization background

Konstantin Y. Guslienko,[1,2,*] Gloria R. Aranda,[3] and Julian M. Gonzalez[1]
[1]*Departamento Fisica de Materiales, Universidad del Pais Vasco, 20018 Donostia-San Sebastian, Spain*
[2]*IKERBASQUE, The Basque Foundation for Science, 48011 Bilbao, Spain*
[3]*Centro de Fisica de Materiales del CSIC-UPV/EHU, Universidad del Pais Vasco, 20018 Donostia-San Sebastian, Spain*
(Received 9 December 2009; published 21 January 2010)

We introduce a topological gauge vector potential which influences spin-wave excitations over arbitrary nonuniform, slowly moving magnetization background. The time component of the gauge potential plays a principal role in the magnetization dynamics of typical magnetic nanostructures. As an example, we consider spin modes excited in the vortex-state magnetic dots. The vortex—spin-wave interaction is described as a consequence of the gauge field arising due to the moving vortex magnetization. The approach yields a giant frequency splitting of the spin waves having nonzero overlapping with the vortex background mode as well as a finite vortex mass of dynamical origin.

DOI: 10.1103/PhysRevB.81.014414 PACS number(s): 75.40.Gb, 75.40.Mg, 75.75.−c

In the recent years a lot of attention was paid to influence of the gauge fields on semiclassical equations of motion of quantum particles such as electrons in solids.[1] It was shown within the local models of itinerant magnetism[2,3] and *s-d* exchange interaction[4] that a topological gauge field induced by a nonuniform magnetization acts on electron motion as a real external magnetic or electric field.[5] From the other side, spin-polarized electric current can essentially contribute to the equation of motion of magnetization[6] transferring angular momentum. The conception of such gauge field has led to prediction and explanation of various observable magnetoelectric effects in patterned nanostructures related to spin angular momentum transfer (spin-Hall effect, magnetoresistance, spin pumping, domain-wall dynamics, etc.), for recent review see Ref. 1 and references therein.

Precise knowledge of the dynamic processes in patterned nanomagnetic materials is important due to their applications in magnetic storage media, magnetic sensors, spintronic devices including microwave nano-oscillators,[7] etc. Understanding dynamic response of nanomagnets to external magnetic field[8,9] or spin-polarized current[10,11] involves rich underlying fundamental physics. Among the different patterned magnetic structures considered so far, flat ferromagnetic particles (dots) with submicron lateral sizes occupy a special place due to their unique, nonuniform vortex ground state.[12] Regular arrays of such dots are being considered as a new high-density nonvolatile recording media[13] characterized by two Boolean variables: chirality and polarity of magnetic vortex core.[12] Special interest in the vortex core, small area where magnetization deviates from the dot plane ($\sim$10–15 nm in size[14]), is inspired by the possibility of easy and fast switching its magnetization direction.[15,16] The vortex-state dots as well as domain walls in magnetic nanostripes[5,11] represent the simplest patterned nanosystems with topologically nontrivial magnetization distribution. However, there is still lack of understanding of the spin-wave dynamics in such strongly nonuniform ground states. The energy dissipation of moving one-dimensional domain wall in bulk anisotropic ferromagnet due to interaction with thermal magnons was considered in Ref. 17 in the rigid domain-wall approximation. The rotation to the local quantization axis related to the domain-wall magnetization direction was used in these papers. But the topological gauge field related to the coordinate transformation was not introduced there.

In this paper we present a gauge potential approach to description of the spin-wave (SW) modes excited over arbitrary nonuniform slowly moving background magnetization distribution $\mathbf{M}_v$. It is shown that a coordinate transformation to the local quantization axis directed along $\mathbf{M}_v$ allows introducing a topological gauge potential, which leads to $\mathbf{M}_v$-SW interaction even in the linear regime of small amplitude spin excitations.

Let us consider a ferromagnetic body with a time-dependent magnetization field $\mathbf{M}(\mathbf{r},t)$ defined in the point $\mathbf{r}$. Assuming conservation of magnetization vector length $|\mathbf{M}|=M_s$ it is convenient to introduce the reduced magnetization $\mathbf{m}=\mathbf{M}/M_s$, $\mathbf{m}^2=1$. To describe $\mathbf{M}$ dynamics we use the Lagrangian Λ corresponding to the Landau-Lifshitz equation of motion of $\mathbf{m}$,

$$\Lambda = \int d^3\mathbf{r}\lambda(\mathbf{r},t), \quad \lambda = \mathbf{D}(\mathbf{m})\cdot\dot{\mathbf{m}} - w(\mathbf{m},\partial_\alpha\mathbf{m}), \qquad (1)$$

where $\mathbf{D}(\mathbf{m})=(M_s/\gamma)(1+\mathbf{m}\cdot\mathbf{n})^{-1}[\mathbf{n}\times\mathbf{m}]$ is the vector potential related to the Dirac string in the direction of an arbitrary unit vector $\mathbf{n}$,[18] the dot over symbol means derivative with respect to time (t), w is the magnetic energy density $w=A(\partial_\alpha\mathbf{m})^2+w_m+w_H$ ($\alpha=x,y,z$), $w_m=-M_s\mathbf{m}\cdot\mathbf{H}_m/2$ is the magnetostatic energy density, $w_H=-M_s\mathbf{m}\cdot\mathbf{H}$ is the Zeeman energy density, A is the exchange stiffness, $\mathbf{H}_m$ and $\mathbf{H}$ are the magnetostatic and external fields.

We distinguish two subsystems in the body: slowly moving magnetization (e.g., a vortex or a domain wall, characteristic time of motion is $\sim$10 ns) plus fast magnetization oscillations described as spin waves (with period about of 0.1 ns) and express magnetization as a sum $\mathbf{m}=\mathbf{m}_v+\mathbf{m}_s$ of the slow magnetization (v) and spin wave (s) contributions. The SW length can be comparable with a characteristic size of $\mathbf{m}_v$ nonuniformity. The damping of the spin excitations

and corresponding transient spin dynamics are not considered here. We assume that the damping is small enough to have well-defined spin excitations. Recalling the restriction $\mathbf{m}^2=1$ the components of $\mathbf{m}_s$ are the simplest in a moving coordinate frame $x'y'z'$, where the axis Oz' is directed along the instant local direction of $\mathbf{m}_\nu$. Therefore, it is convenient to consider dynamics of the fast s subsystem with the quantization axis to be parallel to the slow ν-subsystem magnetization $\mathbf{m}_\nu$ [this is similar to adiabatic approximation used in the spin momentum transfer model[1] when the spins of conductive s electrons can instantly follow the variable magnetization $\mathbf{M}(\mathbf{r},t)$ direction of d electrons]. Then, we perform a rotation of the initial xyz coordinate system to the direction of $\mathbf{m}_\nu$. The corresponding 3×3 real rotation matrix $R(\Theta_\nu,\Phi_\nu)=\exp(i\Phi_\nu J_z)\exp(i\Theta_\nu J_y)$ is defined by the spherical angles of $\mathbf{m}_\nu(\Theta_\nu,\Phi_\nu)$, and $\mathbf{m}_s$ components in new coordinate system are $\mathbf{m}_s'=R\mathbf{m}_s$, $\mathbf{m}_\nu'=(0,0,1)$. Here J_α are the angular momentum components for $J=1$ in the Cartesian basis representation (pure imaginary). To preserve Lagrangian (1) in the same form after transformation $\mathbf{m}\rightarrow\mathbf{m}'=R\mathbf{m}$ we need to introduce covariant derivatives $(\partial_\mu-A_\mu)$ instead ∂_μ, where A_μ is a gauge vector potential (the index $\mu=0$, 1, 2, and 3 denotes the time and space coordinates $x_\mu=t$, x, y, and z, and $\partial_\mu=\partial/\partial x_\mu$). The A_μ components are transformed as $A_\mu\rightarrow A_\mu'=RA_\mu R^{-1}+\partial_\mu R\cdot R^{-1}$. The term $\partial_\mu R\cdot R^{-1}$ has sense of a topological contribution to the vector potential related to the "inertial" moving frame $x'y'z'$. We denote it as $\hat{A}_\mu=\partial_\mu R\cdot R^{-1}$ and put $A_\mu=0$ in the laboratory coordinate system xyz. $\hat{A}_\mu$ acts on the SW magnetization and can be explicitly represented by the time and spatial derivatives of the angles (Θ_ν,Φ_ν) as

$$\hat{A}_\mu=\begin{pmatrix} 0 & \partial_\mu\Phi_\nu & -\cos\Phi_\nu\partial_\mu\Theta_\nu \\ -\partial_\mu\Phi_\nu & 0 & -\sin\Phi_\nu\partial_\mu\Theta_\nu \\ \cos\Phi_\nu\partial_\mu\Theta_\nu & \sin\Phi_\nu\partial_\mu\Theta_\nu & 0 \end{pmatrix}, \quad (2)$$

The skew-symmetric matrix of the operator $\hat{A}_\mu$ can be represented as $\hat{A}_\mu=A_\mu^\alpha\hat{G}_\alpha$ by the generators $\hat{G}_\alpha$ of SO(3) group of three-dimensional rotations, which are expressed in the Cartesian basis as $(\hat{G}_\alpha)_{\beta\gamma}=\varepsilon_{\alpha\beta\gamma}$, $\hat{\varepsilon}$ is the unit antisymmetric tensor, α, β, $\gamma=x$, y, and z. There is a simple equation $\hat{A}_\mu\mathbf{m}=\mathbf{A}_\mu\times\mathbf{m}$ for arbitrary vector $\mathbf{m}$ due to definition of the operator $\hat{A}_\mu$, where $\mathbf{A}_\mu=(\sin\Phi_\nu\partial_\mu\Theta_\nu, -\cos\Phi_\nu\partial_\mu\Theta_\nu, -\partial_\mu\Phi_\nu)$. The gauge vector potential $\hat{A}_\mu$ defined by Eq. (2) introduces a "minimal" interaction between the ν and s subsystems and can be applied to a wide class of problems related to excitation of the SW in the nonuniform magnetization ground state. The first, kinetic, term of Lagrangian (1) can be written in the frame $x'y'z'$ as $\lambda_{kin}=\mathbf{D}'\cdot(\dot{\mathbf{m}}_s'-\hat{A}_0\mathbf{m}_s')$, where the term $\lambda_{\text{int}}=-\mathbf{D}'\cdot\hat{A}_0\mathbf{m}_s'$ corresponds to the dynamic ν—SW interaction. The component $\hat{A}_0(\mathbf{r},t)$ is always important for spin dynamics, but it was neglected in Refs. 19 and 20 because the authors considered only static $\mathbf{m}_\nu$ configurations, where $\hat{A}_\alpha$ appear in the exchange energy terms related to the spatial derivatives $\partial/\partial x_\alpha$. Moreover, in the case of body sizes $\gg L_e$ ($L_e=\sqrt{2A}/M_s\sim10$ nm is the exchange length), $\hat{A}_0$ dominates over other components of $\hat{A}_\mu$ because all the exchange energy terms in the energy density w, Eq. (1), including the spatial derivatives can be neglected. The exchange terms are proportional to the ratio $(L_e/R)^2$ (R is in-plane particle size) and are very small for $R\gg L_e$. The dependence on z coordinate can be neglected for thin magnetic elements. Whereas, the component $\hat{A}_0\propto\dot{\Theta}_\nu,\dot{\Phi}_\nu$ determined by the magnetostatic fields is not, in general, small ($\dot{\Theta}_\nu,\dot{\Phi}_\nu$ satisfy the Landau-Lifshitz equation of motion). This situation is opposite to one in the theory of spin momentum transfer, where the gauge interaction of spin-polarized current with d-electrons spin texture is determined by the spatial derivatives of magnetization.[1,4]

Lagrangian (1) then can be rewritten in the form $\Lambda=\Lambda_\nu+\Lambda_{\text{SW}}+\Lambda_{\text{int}}$, where $\Lambda_{\text{int}}=\int d^3\mathbf{r}\lambda_{\text{int}}$ is the interaction term between the slowly moving nonuniform magnetization $\mathbf{m}_\nu$ (we briefly call such structure as "soliton") described by the Lagrangian Λ_ν and spin waves, which are described by the Lagrangian density $\lambda_{\text{SW}}=\mathbf{D}'\cdot\dot{\mathbf{m}}_s'-w(\mathbf{m}_s',\partial_\alpha\mathbf{m}_s')$. There always exist some SW of a specific symmetry on the moving soliton background, which strongly interact with the soliton and renormalize their frequencies. From the other side, this interaction results in appearing of the soliton dynamic mass, soliton profile distortions, and eventually, increasing the SW intensity (the soliton velocity), leads to its dynamical instability, like the vortex-core reversal or the Walker instability of moving domain walls.

To demonstrate how useful and powerful the approach based on the potential $\hat{A}_\mu$ is, we apply this formalism to the problem of coupled vortex—SW motion in submicron size cylindrical dots in the vortex state. Magnetic dot with the vortex core possesses two qualitatively different kinds of spin excitation modes: the lowest in frequency gyrotropic mode (GM, typically several 100 MHz) localized near the dot center[9,21] and high-frequency (several gigahertz) spin waves.[9,10,22] The excited mainly outside the vortex-core SW modes are described by integers (n,m), which indicate number of nodes in the dynamic magnetization along radial (n) and azimuthal (m) directions. For in-plane magnetic driving field the azimuthal SW and GM mode $(m=\pm1)$ with nonzero dipolar moments can be only excited.[8,9,23] The azimuthal SW with $m=\pm1$ having the same symmetry as the vortex background GM are especially important because they are responsible for the vortex-core distortion resulting in the core switching.[15]

The component $A_\mu^z=-\partial_\mu\Phi_\nu$ of the vector $\mathbf{A}_\mu$ plays crucial role in the dynamics, whereas the other components of $\mathbf{A}_\mu\sim\partial_\mu\Theta_\nu$, related to the vortex core (the area where $\Theta_\nu\neq\pi/2$), can be neglected in the main approximation. The vector potential $\hat{A}_\mu$ leads to essential renormalization of the azimuthal SW spectra and appearance of a dynamical vortex mass induced by the SW-vortex interaction. For typical dot sizes (the thickness $L\sim10$ nm, the radius $R\sim500$ nm) influence of the exchange interaction on dynamics can be neglected. We also assume that $\mathbf{m}$ does not depend on z coordinate along the dot thickness L. The vortex magnetization $\mathbf{m}_\nu(\boldsymbol{\rho},t)=\mathbf{m}_\nu[\boldsymbol{\rho},\mathbf{X}(t)]$ can be characterized by its core coordinate $\mathbf{X}=(X,Y)$, velocity, etc., within the collective-variable approach.[21] The unperturbed vortex Lagrangian is $\Lambda_\nu(\mathbf{X},\dot{\mathbf{X}})$

$=(\mathbf{G}\times\mathbf{X})\cdot\dot{\mathbf{X}}/2-W(\mathbf{X})$, where $W(\mathbf{X})$ is the energy of the vortex shifted from its equilibrium position at $\mathbf{X}=0$ ($\mathbf{H}=0$), $\mathbf{G}=\hat{\mathbf{z}}2\pi pLM_s/\gamma$ is the gyrovector, γ is the gyromagnetic ratio, $\hat{\mathbf{z}}$ is the unit vector perpendicular to the dot plane xOy, and p is the vortex-core polarization.

To derive magnetic vortex and SW dynamics from the Lagrangian Λ we use a quadratic approximation in small spin excitation amplitudes and consider linear coupled equations of motion of the system "vortex+SW." The vector $\mathbf{m}(\boldsymbol{\rho},t)$ [$\boldsymbol{\rho}=(x,y)$] maps the xOy plane to the surface of unit sphere $\mathbf{m}^2=1$. Therefore, we use the angular parameterization for the dot $\mathbf{m}$ components, $m_z=\cos\Theta$, $m_x+im_y=\sin\Theta\exp(i\Phi)$ in the xyz frame. Moving $\mathbf{m}(\boldsymbol{\rho},t)$ is expressed by the angles $\Theta(\boldsymbol{\rho},t)=\Theta_v(\boldsymbol{\rho},t)+\vartheta(\boldsymbol{\rho},t)$, $\Phi(\boldsymbol{\rho},t)=\Phi_v(\boldsymbol{\rho},t)+\psi(\boldsymbol{\rho},t)$, where the variables Θ_v, Φ_v describe the moving vortex $\mathbf{m}_v$, and $\mathbf{m}_s'=(m_{x'}^s,m_{y'}^s,0)=(\vartheta,\psi,0)$ describes SW excitations. The $\mathbf{m}_s'$ components are used in the form $\vartheta(\boldsymbol{\rho},t)=a_n(\rho)\cos(m\varphi-\omega t)$, $\psi(\boldsymbol{\rho},t)=b_n(\rho)\sin(m\varphi-\omega t)$, where a_n, b_n are the SW amplitudes, $n=0,1,2,\ldots$, $m=0,\pm1,\pm2,\ldots$, ρ,φ are the polar coordinates. Due to small core size the contribution of the vortex-core region to $\mathbf{m}_v$ and SW magnetization $\mathbf{m}_s'$ is also small. The dynamic vortex-SW coupling induced by the component $\hat{A}_0$ exists only for the azimuthal modes with the indices $m=\pm1$, which have the same angular dependence as the vortex GM, and is considered below.

The SW Lagrangian density in our case is $\lambda_{\mathrm{SW}}=(M_s/\gamma)\vartheta\dot{\psi}+M_s\mathbf{m}_s\cdot\mathbf{H}_m$ and the interaction Lagrangian density is the bilinear form $\lambda_{\mathrm{int}}=(M_s/\gamma)\sin\Theta_v\dot{\Phi}_v\vartheta$ in the vortex and SW excitation amplitudes. Note that λ_{int} is reduced to the form suggested by Slonczewski for infinite films.[24] We get a system of four coupled equations of motion: two integral equations for the SW variables ϑ, ψ (neglecting the exchange interaction), and two differential ones for the vortex variables $\mathbf{X}=(X,Y)$. The latter are reduced to the Thiele's equation with an extra force $\dot{\mathbf{P}}$ due to the SW field momentum $\mathbf{P}=(M_sL/\gamma)\int d^2\boldsymbol{\rho}\sin\Theta_0\vartheta\nabla_{\mathbf{X}}\Phi_v$,

$$\mathbf{G}\times\dot{\mathbf{X}}+\partial_{\mathbf{X}}W=-\dot{\mathbf{P}}[\vartheta], \tag{3}$$

while the former are

$$\dot{\vartheta}=-\gamma H_m^{\rho},\quad \dot{\psi}=\gamma H_m^{z}-\dot{\Phi}_v, \tag{3'}$$

where $\mathbf{H}_m(\boldsymbol{\rho},t)=M_s\int d^2\boldsymbol{\rho}'\hat{G}(\boldsymbol{\rho},\boldsymbol{\rho}')\mathbf{m}_s(\boldsymbol{\rho}',t)$ is the dynamic magnetostatic field, the kernel $(\hat{G})_{\alpha\beta}=G_{\alpha\beta}(\boldsymbol{\rho},\boldsymbol{\rho}')$ is the averaged over thickness magnetostatic tensor,[25] $\alpha,\beta=\rho,\varphi,z$, and $\Theta_0(\rho)$ is the static vortex profile.

There is an essential contribution to the SW motion in Eq. (3′) due to the variable vortex phase $\dot{\Phi}_v=-A_0^z$ (we note that $-\dot{\Phi}_v/\gamma$ is z component of the dynamical vortex gyrofield,[26] which is created by the moving vortex core). Spatial dependence of $\hat{A}_0$ is important and contributes to Eqs. (3) and (3′). $\dot{\Phi}_v$ can be calculated, for instance, by the vortex pole free model[21] to be $\dot{\Phi}_v=m_0(\rho)[\dot{X}\sin\varphi-\dot{Y}\cos\varphi]$, where $m_0(\rho)=(1-\rho^2)/\rho$ is the radial profile of the vortex GM mode defined in Ref. 22 within the standard spin-wave approach, ρ is in units of R.

The spin eigenfrequencies/eigenfunctions in presence of the vortex core can be found expressing the solution of the equation for $\mathbf{X}(t)$, Eq. (3), via the s variables. Then the solution of Eq. (3) is substituted to Eq. (3′) forming the closed system of equations for the spin-wave amplitudes $a_n(\rho),b_n(\rho)$. Excluding the variable ψ we get from Eq. (3′) the inhomogeneous linear integral equation for ϑ in the approximation $\beta=L/R\ll1$,

$$\ddot{\vartheta}-\frac{\omega_M^2}{4\pi}\int d^2\boldsymbol{\rho}'G_{\rho\rho}(\boldsymbol{\rho},\boldsymbol{\rho}')\vartheta(\boldsymbol{\rho}',t)=\omega_M[\dot{X}\sin\varphi-\dot{Y}\cos\varphi]F(\rho), \tag{4}$$

where $\omega_M=\gamma4\pi M_s$, $F(\rho)=\delta_{|m|,1}\int_0^1 d\rho'\rho' g(\rho,\rho')m_0(\rho')$, and $g(\rho,\rho')=-\int d\varphi' G_{\rho\rho}(\boldsymbol{\rho},\boldsymbol{\rho}')/4\pi$.[25]

To find radial parts of the SW variables ϑ and ψ without interaction with the vortex core ($\dot{\Phi}_v=0$), Eq. (4) is reduced to eigenvalue problem for the integral magnetostatic operator[25] with kernel $g(\rho,\rho')$ and a discrete set of (n,m)-magnetostatic eigenfunctions and corresponding SW eigenfrequencies ω_{nm} [ω_{nm} are proportional to $(L/R)^{1/2}$ for thin dots] can be calculated. The eigenfrequencies are degenerated with respect to sign of m and are well above the gyrotropic eigenfrequency, ω_0.[12]

The inhomogeneous right-hand part of Eq. (4), where integration over the azimuthal angle φ' was performed, depends explicitly on $\dot{\mathbf{X}}$. As the first step, the inhomogeneous vortex-core equation of motion, Eq. (3), for X and Y is solved, i.e., its particular solution is represented via spin-wave variables. The time derivatives of the vortex-core coordinates $\dot{X},\dot{Y}$ calculated from Eq. (3) are proportional to the azimuthal index m, and, therefore, the right-hand side of Eq. (4) for the spin-wave variable ϑ is also proportional to m. This leads to splitting of the azimuthal SW eigenfrequncies obtained as solution of Eq. (4) due to different signs of the index $m=+1/-1$ and yields the perturbed azimuthal SW frequencies $\omega_{nm}'=\omega_{n1}+m\Delta\omega_n/2$ ($m=\pm1$) and SW eigenmodes. The frequency splitting is $\Delta\omega_n=p\mathfrak{I}_n^2\omega_{n1}^2/2\omega_M$, where $\mathfrak{I}_n=\int d\rho\rho m_0(\rho)a_n(\rho)$ is the overlapping integral of the vortex GM $m_0(\rho)$ and the unperturbed eigenmode $a_n(\rho)$ obtained from solution of homogeneous Eq. (4), normalized to unit, and ω_{n1} are the eigenvalues of the homogeneous Eq. (4). $\mathfrak{I}_n$ and $\Delta\omega_n$ are especially large for the main SW mode $n=0$ reaching 1.6 and ~2 GHz for $\beta=0.1$, and they rapidly decrease with n increasing (Fig. 1). That allows calculating the splitting $\Delta\omega_n$ for arbitrary n, whereas where only $n=0$ was considered in Ref. 22. The calculated values $\Delta\omega_0=1.11$ GHz, $\Delta\omega_1=0.99$ GHz for $\beta=0.048$ with the parameters listed in Ref. 27 are in good agreement with the broadband ferromagnetic resonance measurements,[23] where $\Delta\omega_0=0.87$ GHz, $\Delta\omega_1=0.80$ GHz were detected for permalloy dots with $L=25$ nm, $R=518$ nm. The SW mode spatial distributions and accuracy of the expression for $\Delta\omega_n$ were checked numerically.[27] Three resonance peaks of the magnetization response to external in-plane variable field were ob-

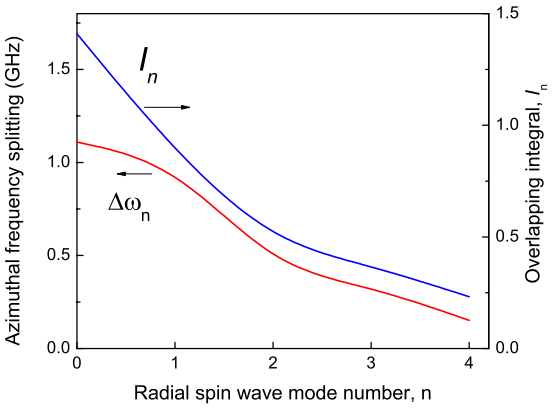

FIG. 1. (Color online) Dependence of the spin-mode overlapping integral $\mathfrak{I}_n$ and azimuthal ($m=\pm 1$) spin-wave frequency splitting $\Delta\omega_n$ on the radial mode number n. The dot aspect ratio is $\beta=0.048$, other parameters are as in Ref. 27.

tained in the frequency range 0–12 GHz: at 0.48 GHz (GM) and at 8.98 and 10.44 GHz, which correspond to the azimuthal SW ($n=0; m=\pm 1$) traveling counterclockwise and clockwise, respectively. From these simulations we extracted the spatial distributions of the dynamic magnetization component $m^s_{y'}(\boldsymbol{\rho},t)$ for selected times (Fig. 2). The spatial distributions evidence essential difference between the ($m=\pm 1$) azimuthal SW modes due to strong hybridization with GM: the low-frequency SW mode has radial profile with no nodes and a peak close to the dot center, whereas the high-frequency mode except the peak near the core has maximum amplitude in the middle of the dot and a node. The presented equation for $\Delta\omega_n$ slightly overestimates the azimuthal SW frequency splitting value, mainly due to neglecting an intermode dynamical dipolar interaction. We note that the presented micromagnetic simulations including both the exchange and magnetostatic interactions for realistic dot sizes ($L=10$ nm and $R=100$ nm) yield qualitatively similar results for the azimuthal spin-wave mode profiles with indices $m=+1/-1$ as compared with the calculated profiles in the paper by Ivanov *et al.*,[28] where an anisotropic exchange two-dimensional (2D) model was used. The exchange model[28] is not realistic for magnetic dots of finite thickness having the considerable magnetostatic interaction. It is clear from the profiles in Fig. 2 that the spin eigenmodes satisfy neither free nor strong pinning boundary conditions at $\rho=R$ as it was assumed in Ref. 28. The pinning is relatively weak and can be calculated from Eq. (8) in Ref. 12.

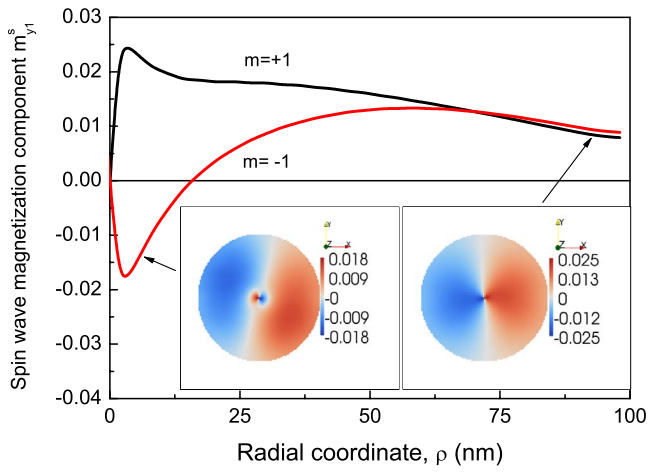

FIG. 2. (Color online) The radial profiles of the main (the radial index $n=0$, $m=\pm 1$) azimuthal spin waves in the vortex state dot with $p=-1$. The eigenmode frequencies are $\omega_{0,+1}/2\pi=8.98$ GHz and $\omega_{0,-1}/2\pi=10.44$ GHz for the azimuthal indices $m=+1$ and $m=-1$, respectively. Inset: snapshots of the dynamic $m^s_{y'}$-magnetization component. The dot aspect ratio is $\beta=0.1$, other parameters are as in Ref. 27.

From the other side, expressing the solution of the inhomogeneous SW equation of motion (4) via $\mathbf{X}$ and substituting it to $\Lambda_{\text{int}}=\mathbf{P}\cdot\dot{\mathbf{X}}$ we get the formula $\Lambda_{\text{int}}=M_{\alpha\beta}\dot{X}_\alpha\dot{X}_\beta/2$, where $M_{\alpha\beta}=M\delta_{\alpha\beta}$ is the tensor of a vortex mass having the diagonal components $M=-L/(2\gamma^2)\int d\rho\rho \sin\Theta_0 m_0 a$. Solving Eq. (4) we get $a(\rho)=-\Sigma_n\mathfrak{I}_n a_n(\rho)$ in the limit $\omega_0\ll\omega_{n1}$. The vortex mass has the simple form $M=L/(2\gamma^2)\Sigma_n\mathfrak{I}_n^2$ evidencing its dynamical origin [$M\approx(3/2)L/\gamma^2$ and is about 10^{-20} g, being comparable with the transverse domain-wall mass 6.6×10^{-20} g measured in Ref. 29 or the vortex domain wall mass 6.2×10^{-21} g measured in Ref. 30]. All the azimuthal SW with the indices ($n, m=\pm 1$) contribute to M. Therefore, the effective vortex Lagrangian is $\Lambda_v^{eff}(\mathbf{X},\dot{\mathbf{X}})=M(\dot{\mathbf{X}})^2/2+(\mathbf{G}\times\mathbf{X})\cdot\dot{\mathbf{X}}/2-W(\mathbf{X})$. It leads to the gyrotropic frequency $\omega_0'=\omega_0(1-\omega_0 M/|\mathbf{G}|)$, where the mass correction is always negative for any form of the dependence $\omega_0(\beta)$. The correction is relatively small at $\beta\ll 1$ but essentially contributes to the deviations from the linear behavior $\omega_0'(\beta)\propto\beta$ increasing β observed in Ref. 21. The mass contribution to nonlinearity of the resulting function $\omega_0'(\beta)$ is approximately 2/3 of the nonlinearity of the function $\omega_0(\beta)$ itself. Accounting the expression $M\approx(3/2)L/\gamma^2$, the gyrotropic frequency is $\omega_0'(\beta)=\omega_0(\beta)[1-3\omega_0(\beta)/\omega_M]$ or using explicitly the dependence $\omega_0(\beta)$ (Ref. 12) it can be represented in the form $\omega_0'(\beta)=\omega_M(5/9\pi)\beta[1-4\beta/3]$ at small $\beta\leq 0.2$. The vortex kinetic-energy term (the mass) corresponds to increase in the moving vortex energy increasing its velocity and can be interpreted as result of the dynamic vortex profile distortion investigated in details in Refs. 26 and 31. The vortex-core distortion due to self-induced gyrofield can be represented as a result of the hybridization of the GM with azimuthal SW and leads to the core polarization reversal at a critical velocity. The corresponding instability field of the reversal was calculated in the linear approximation on the spin excitation amplitudes. All nonlinearities accounted numerically in Ref. 31 did not change considerably the critical parameters calculated from the linear approach using the conception of the vortex-core critical velocity.

We note that the spin dynamics in the vortex ground state was calculated within anisotropic Heisenberg exchange 2D model (the magnetic element thickness and magnetostatic interaction is ignored in this model).[28,32] The dynamical character of the vortex mass, which is a property of the whole system "vortex plus spin waves" was understood using this 2D model.[28,32] But the anisotropic exchange 2D model is not realistic for patterned magnetic nanostructures with dominating magnetostatic interaction. For instance, the

vortex mass M proportional to the system in-plane size R was calculated in Ref. 32 numerically from 2D Heisenberg model. The mass M independent on the system sizes was calculated in Ref. 28. Whereas the present calculation yields the vortex mass proportional to the dot thickness L. Despite of the small value of the vortex mass, there are some cases, for instance, the vortex domain-wall resonance in nanostripes[29] and nanorings[30] when M plays important role in the dynamics.

The dynamic vortex-SW coupling Λ_{int} determined by the time derivatives $\dot{\mathbf{P}}$, $\dot{\Phi}_v$ and expressed via $\mathfrak{I}_n$ exists only for the azimuthal SW modes with $m=\pm 1$ (n is arbitrary). The gauge potential $\hat{A}_0$ generated by the moving vortex results in the giant frequency splitting $\Delta\omega_n$ of the degenerated azimuthal SW and explains naturally the experimental data.[8,9,33] Removing the vortex core from the dot leads to disappearance of the splitting[9,33] proving importance of the core motion represented by the potential component $A_0^z=-\dot{\Phi}_v$. The gauge potential $\hat{A}_\mu$ yields the significant interaction between the v and s subsystems within the linear on spin excitation amplitudes approximation.

In summary, a general approach to description of the small SW excitations of a nonuniform moving magnetization background was developed and applied to particular case of the spin waves excited in the moving vortex state. The slowly moving magnetization background influences the spin waves via a topological gauge vector potential, which is represented by time and spatial derivatives of the nonuniform magnetization. Increasing amplitude of the spin waves leads to an instability of the background. The vortex-SW interaction results in the giant SW frequency splitting as well as in renormalization of the vortex background motion due to appearance of the vortex profile distortion and a finite vortex mass. Other dynamic magnetic nanostructures, e.g., moving domain walls in nanostripes (nanorings) can be considered within the approach.

The authors thank A. K. Zvezdin for fruitful discussions. K.G. and G.R.A. acknowledge support by IKERBASQUE (the Basque Science Foundation) and by the Program JAE-doc of the CSIC (Spain), respectively. The work was partially supported by the SAIOTEK grant S-PC09UN03. The authors thank the Donostia International Physics Center and Centro de Fisica de Materiales for computation tools and technical help.

*Corresponding author; sckguslk@ehu.es

[1] G. Tatara, H. Kohno, and J. Shibata, Phys. Rep. **468**, 213 (2008).
[2] V. Korenman, J. L. Murray, and R. E. Prange, Phys. Rev. B **16**, 4032 (1977); **16**, 4058 (1977); V. Korenman and R. E. Prange, J. Appl. Phys. **50**, 1779 (1979).
[3] G. E. Volovik, J. Phys. C **20**, L83 (1987).
[4] G. Tatara, H. Kohno, J. Shibata, Y. Lemaho, and K. Lee, J. Phys. Soc. Jpn. **76**, 054707 (2007).
[5] S. A. Yang, G. S. D. Beach, C. Knutson, D. Xiao, Q. Niu, M. Tsoi, and J. L. Erskine, Phys. Rev. Lett. **102**, 067201 (2009).
[6] L. Berger, Phys. Rev. B **54**, 9353 (1996); J. Slonczewski, J. Magn. Magn. Mater. **159**, L1 (1996).
[7] M. R. Pufall, W. H. Rippard, S. E. Russek, S. Kaka, and J. A. Katine, Phys. Rev. Lett. **97**, 087206 (2006).
[8] J. P. Park and P. A. Crowell, Phys. Rev. Lett. **95**, 167201 (2005).
[9] X. Zhu, Z. Liu, V. Metlushko, P. Grutter, and M. R. Freeman, Phys. Rev. B **71**, 180408(R) (2005).
[10] V. S. Pribiag, I. N. Krivorotov, D. G. Fuchs, P. M. Braganca, O. Ozatay, J. C. Sankey, D. C. Rlaph, and R. A. Buhrman, Nat. Phys. **3**, 498 (2007).
[11] M. Hayashi, L. Thomas, C. Rettner, R. Moriya, and S. S. P. Parkin, Nat. Phys. **3**, 21 (2007).
[12] K. Yu. Guslienko, J. Nanosci. Nanotechnol. **8**, 2745 (2008).
[13] S.-K. Kim, K.-S. Lee, Y. S. Yu, and Y. S. Choi, Appl. Phys. Lett. **92**, 022509 (2008).
[14] A. Wachowiak, J. Wiebe, M. Bode, O. Pietzsch, M. Morgenstern, and R. Wiesendanger, Science **298**, 577 (2002).
[15] B. Van Waeyenberge, A. Puzic, H. Stoll, K. W. Chou, T. Tyliszczak, R. Hertel, M. Fahnle, H. Bruckl, K. Rott, G. Reiss, I. Neudecker, D. Weiss, C. H. Back, and G. Schutz, Nature (London) **444**, 461 (2006).
[16] S. Choi, K.-S. Lee, K. Yu. Guslienko, and S.-K. Kim, Phys. Rev. Lett. **98**, 087205 (2007).
[17] A. S. Abyzov and B. A. Ivanov, Sov. Phys. JETP **49**, 865 (1979); B. A. Ivanov, Yu. N. Mitsai, and N. V. Shakhova, *ibid.* **60**, 168 (1984).
[18] P. A. M. Dirac, Proc. R. Soc. London **133**, 60 (1931); Phys. Rev. **74**, 817 (1948).
[19] D. D. Sheka, I. A. Yastremsky, B. A. Ivanov, G. M. Wysin, and F. G. Mertens, Phys. Rev. B **69**, 054429 (2004).
[20] V. K. Dugaev, P. Bruno, B. Canals, and C. Lacroix, Phys. Rev. B **72**, 024456 (2005).
[21] K. Y. Guslienko, B. A. Ivanov, V. Novosad, H. Shima, Y. Otani, and K. Fukamichi, J. Appl. Phys. **91**, 8037 (2002); V. Novosad, F. Y. Fradin, P. E. Roy, K. Buchanan, K. Y. Guslienko, and S. D. Bader, Phys. Rev. B **72**, 024455 (2005).
[22] K. Y. Guslienko, A. N. Slavin, V. Tiberkevich, and S.-K. Kim, Phys. Rev. Lett. **101**, 247203 (2008).
[23] F. G. Aliev, J. F. Sierra, A. A. Awad, G. N. Kakazei, D.-S. Han, S.-K. Kim, V. Metlushko, B. Ilic, and K. Y. Guslienko, Phys. Rev. B **79**, 174433 (2009); A. A. Awad, K. Y. Guslienko, J. F. Sierra, G. N. Kakazei, V. Metlushko, and F. G. Aliev, Appl. Phys. Lett. **96**, 012503 (2010).
[24] J. C. Slonczewski, in *Physics of Magnetic Materials*, edited by J. Rauluszkiewicz, H. Szymczak, and H. K. Lachowicz (World Scientific, Singapore, 1985).
[25] K. Y. Guslienko and A. N. Slavin, J. Appl. Phys. **87**, 6337 (2000).
[26] K. Y. Guslienko, K.-S. Lee, and S.-K. Kim, Phys. Rev. Lett. **100**, 027203 (2008).
[27] We used the OOMMF code: http://math.nist.gov/oommf/bibliography.html. We simulated a permalloy dot with radius $R=100$ nm and thickness $L=10$ nm using the exchange constant $A=13$ pJ/m, the saturation magnetization $M_s=800$ kA/m, the

Gilbert damping constant $\alpha=0.01$, the gyromagnetic ratio $\gamma/(2\pi)=2.95$ MHz/Oe, zero anisotropy constant, and cell size $2\times2\times10$ nm.

[28] B. A. Ivanov, H. J. Schnitzer, F. G. Mertens, and G. M. Wysin, Phys. Rev. B **58**, 8464 (1998).

[29] E. Saitoh, H. Miajima, T. Yamaoka, and G. Tatara, Nature (London) **432**, 203 (2004).

[30] D. Bedau, M. Klaui, S. Krzyk, U. Rudiger, G. Faini, and L. Vila, Phys. Rev. Lett. **99**, 146601 (2007); D. Bedau, M. Klaui, M. T. Hua, S. Krzyk, U. Rudiger, G. Faini, and L. Vila, *ibid.* **101**, 256602 (2008).

[31] K.-S. Lee, S.-K. Kim, Y. S. Yu, Y. S. Choi, K. Y. Guslienko, H. Jung, and P. Fischer, Phys. Rev. Lett. **101**, 267206 (2008).

[32] G. M. Wysin, Phys. Rev. B **54**, 15156 (1996).

[33] F. Hoffmann, G. Woltersdorf, K. Perzlmaier, A. N. Slavin, V. S. Tiberkevich, A. Bischof, D. Weiss, and C. H. Back, Phys. Rev. B **76**, 014416 (2007).